

Integral model of shallow mixing layers

Modèle intégral de couches de mélange peu profondes

ROBERT BOOIJ, *Faculty of Civil Engineering and Geosciences, Hydromechanics Section, Delft University of Technology, P.O. Box 5048, 2600 GA Delft, The Netherlands, E-mail: r.booi@ct.tudelft.nl.*

JAN TUKKER, *Faculty of Civil Engineering and Geosciences, Hydromechanics Section, Delft University of Technology, The Netherlands. Present address: MARIN, P.O. Box 28, 6700 AA Wageningen, The Netherlands.*

ABSTRACT

Mixing layers that develop downstream of the confluence between two flows of different velocity determine the lateral exchange of pollutants and sediment between both flows. The shallowness of most flows in the natural environment restricts the development of those mixing layers in two ways. First, the bottom friction has a stabilizing influence on the generation of large-scale turbulent structures in the mixing layer and in this way reduces the growth of the mixing layer. Second, the bottom friction leads to a decrease of the velocity difference between both flows, also leading to a reduced growth. This reduced growth results in a reduced lateral exchange between both flows which has consequences for the pollution and sedimentation of harbours and flood plains and for the longitudinal dispersion in rivers. To predict the development of mixing layers in shallow flows a simple integral model was developed in which both reduction mechanisms are incorporated. The model gives a fair reproduction of the downstream evolution of the width and the transverse displacement of investigated shallow mixing layers on laboratory scale. Simulation of river confluences yields very narrow mixing layers which corresponds to the often observed phenomenon that merging rivers hardly mix, but appear to flow alongside each other over a long reach.

RÉSUMÉ

Les couches de mélange qui se développent à l'aval du confluent de deux écoulements de vitesses différentes déterminent l'échange latéral des polluants et des sédiments entre les deux écoulements. La faible profondeur des écoulements dans le milieu naturel limite le développement de ces couches de mélange de deux manières. D'abord le frottement au fond a une influence stabilisante sur la génération des structures turbulentes à grande échelle dans la couche de mélange et cela réduit la croissance de la couche de mélange. En second lieu, le frottement au fond provoque une diminution de la différence des vitesses entre les 2 écoulements, conduisant également à une croissance réduite. Cette croissance réduite entraîne une diminution des échanges latéraux entre les 2 écoulements qui a des conséquences pour la pollution et la sédimentation dans les ports et les plaines d'inondation et pour la dispersion longitudinale en rivière. Afin de prédire le développement des couches de mélange dans les écoulements en faible profondeur, un modèle intégral simple a été développé, dans lequel les 2 mécanismes de réduction sont incorporés. Le modèle reproduit convenablement l'évolution aval de la largeur et du déplacement transversal des couches de mélange en faible profondeur étudiées à l'échelle du laboratoire. La simulation de confluence de rivières donne des couches de mélange très étroites qui correspondent aux phénomènes, souvent observés, de rivières qui convergent en se mélangeant à peine, et semblent couler côte à côte sur une longue distance.

1. Introduction

Turbulent flows in the natural environment are mostly shallow flows, i.e. with large horizontal length scales compared to the water depth. In shallow-water flows the turbulent bottom boundary layer extends through the whole water depth. Recently much attention has been given to the influence of shallowness on lateral transport processes in transverse shear layers: shallow jets (Dracos et al., 1992), shallow wakes behind islands (Lloyd and Stansby, 1997) or other obstructions (Chen and Jirka, 1995), and shallow mixing layers (Chu and Babarutsi, 1988). Lateral mixing layers, the transition zones between contiguous flows of different velocity, intensify the lateral exchange of material and of momentum and so are of importance for the dispersion of pollutants and sediment. Examples of shallow mixing layers can be found for instance in confluences of two rivers, in harbour entrances between the main flow and the flow in the harbour (Langendoen, 1992), in rivers between main flow and flow between groynes or over flood plains (Sellin, 1964, and Knight and Shiono, 1990). Knowledge of mixing layers concerns mostly two-dimensional or plane mixing layers without a spanwise confinement. The velocity difference between both sides of the mixing layer gives rise to

instabilities in the fluid motion resulting in the development of the mixing layer. Long living turbulent structures with the vorticity aligned with the mean flow vorticity are continuously fed from the main flow. These large scale structures which have a length scale of the order of the width of the mixing layer lose energy through the normal energy cascade process to smaller eddies leading to a continuous spectrum of three-dimensional turbulence motions from the large scale structures unto the dissipation range. A plane mixing layer develops in a self-preserving way with a constant spreading rate, depending only on the relative velocity difference across the mixing layer (Townsend, 1976). In shallow flow both the limited depth and the bottom friction influence the development of the mixing layer. The limited depth restricts the large structures in the mixing layer to basically two-dimensional horizontal motions. Because of the shallowness the normal energy cascade from large to small eddies is interrupted (Chu and Babarutsi, 1988). The bottom friction has a two-fold influence on the large-scale structures. First, the bottom friction is responsible for dissipation of large-scale energy which is transferred directly from the large-scales to the small-scales without interaction of intermediate scales. Second, the bottom friction has a stabilizing influence on the generation of large-scale structures

Revision received May 18, 2000. Open for discussion till October 31, 2001.

and therefore reduces the growth of the mixing layer. Extensive experimental research on the turbulence in shallow mixing layers by Tukker (1997) and Uijttewaal and Tukker (1998) has corroborated this picture. The bottom friction in shallow flow reduces the growth of the mixing layer in still another way. Due to the bottom friction the velocity difference across the mixing layer decreases generally, leading to a slower development. The remarkably slow mixing of two rivers downstream of their confluence, which is often observed when the rivers convey water of different colour, is due to this reduced growth of the mixing layer.

The influence of shallowness on the development of mixing layers in environmental flows can be of importance as this development determines for instance the lateral exchange of pollutants and sediment into harbours and onto flood plains and the longitudinal dispersion in rivers. To predict the development of mixing layers in shallow flows of limited width a simple integral model was developed. The model yields the development of the mixing layer width, the water level, the velocities and widths of the two ambient flows and the displacement of the mixing layer centre. An evaluation of the model is based on experiments by Tukker (1997) in a dedicated shallow water flume.

2. Free mixing layer

A free mixing layer is a free turbulent shear flow, a flow in which turbulent transports are determined by internal velocity gradients. The transport processes in a free mixing layer depend on a single length scale, corresponding to the local width of the mixing layer. This presence of a single length scale is a characteristic of self-preserving free shear flows, the evolution of which can be described with self-preserving or self-similar functions.

The free mixing layer considered is a plane shear layer between two parallel streams, a fast stream and a slow stream (see figure 1). The main flow is directed in the longitudinal direction (x), and the gradient of the main flow velocity is in the transverse direction (y). Both ambient streams extend in the direction parallel to the plane of shear, the so-called spanwise direction. Outside the mixing layer the mean velocity u has the value u_1 at the fast stream side and u_2 at the slow stream side, giving a velocity difference $\Delta_u = u_1 - u_2$ across the mixing layer. The centre of the mixing layer, where $y = y_c$, is defined as the position in a cross-

section where the mean velocity is equal to $u_c = \frac{1}{2}(u_1 + u_2)$.

At its origin a free mixing layer is a shear plane between contiguous parallel flows. Small wavy disturbances on this plane develop downstream into large coherent structures. This instability process is called the Kelvin-Helmholtz instability. The width of the free mixing layers corresponds to the dimensions of the large coherent structures. The large-scale coherent structures entrain fluid and momentum into the layer and are in this way mainly responsible for the large transverse exchange of momentum and matter across the mixing layer and for the transverse spreading of the layer. The downstream evolution of a free mixing layer is usually described in terms of the evolution of the width of the layer, defined as the maximum-slope thickness of the mean-velocity profile δ :

$$\delta \equiv \frac{\Delta_u}{(\partial u / \partial y)_{\max}} \quad (1)$$

The subscript \max denotes the maximum value over the profile. A characteristic of self-preserving free mixing layers is a linear spreading. In case of mixing layers in incompressible fluids with uniform density, the spreading rate is proportional to the relative velocity difference λ :

$$\frac{d\delta}{dx} = \alpha \lambda \quad \text{with} \quad \lambda \equiv \frac{u_1 - u_2}{u_1 + u_2} = \frac{\Delta_u}{2u_c} \quad (2)$$

Here λ is the velocity difference across the mixing layer, Δ_u , normalized with twice the mean convection velocity u_c and α is a proportionality parameter, called the spreading coefficient. From spreading rates measured by various investigators, an average value $\alpha=0.18 (\pm 0.015)$ has been obtained (Brown and Roshko, 1974). The spreading rate of a mixing layer is influenced by the turbulence outside the mixing layer. Turbulent ambient streams stimulate the entrainment into the layer resulting in a small increase of the spreading rate of a mixing layer (Pui and Gartshore, 1979).

The linear spread of the mixing layer leads to a linear relation for the width, $\delta = \alpha \lambda (x - x_o)$, in which x is the distance to the origin of the mixing layer, for instance the downstream edge of a splitter plate. A shift x_o is introduced to correct for initial effects, such as

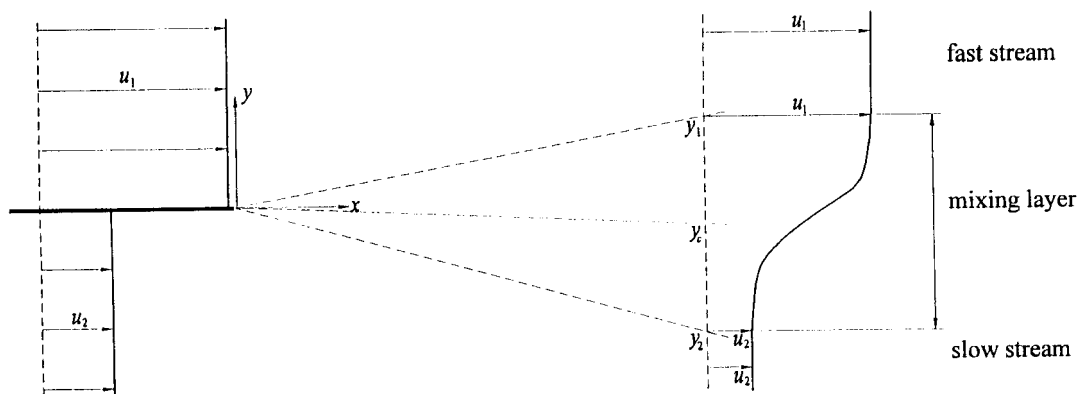


Fig. 1. Scheme of a free mixing layer.

finite thickness of the splitter plate and the influence of the boundary layers along the splitter plate, leading to initial non-similarity.

For free mixing layers the transverse distribution of the mean, longitudinal velocity u can be described with a self-similar profile function $\mathbf{f}(\eta)$:

$$u = u_c + \mathbf{f}(\eta) \Delta_u \quad \text{with} \quad \eta = \frac{y - y_c}{\delta} \quad (3)$$

Here η is a self-similar coordinate, obtained by scaling the transverse coordinate with the maximum-slope thickness δ defined in equation (1) as a transverse length scale. A suitable expression for the self-similar profile function $\mathbf{f}(\eta)$ is the error-function (Görtler, 1942):

$$\mathbf{f}(\eta) = \frac{1}{2} \operatorname{erf}(\eta\sqrt{\pi}) = \frac{1}{\sqrt{\pi}} \int_0^{\eta\sqrt{\pi}} e^{-\tilde{\eta}^2} d\tilde{\eta} \quad (4)$$

The error function is a point-symmetric profile function with $\mathbf{f}(\eta) = -\mathbf{f}(-\eta)$ and $-\frac{1}{2} \leq \mathbf{f}(\eta) \leq \frac{1}{2}$.

3. Shallow mixing layer

In shallow-water flow the confinement of the flow between bottom and free surface restricts the mean flow and large-scale turbulence motions to mainly horizontal motions. This motivates the application of 2D-models using depth-averaged quantities, so-called depth-averaged shallow-water models (see for more details Vreugdenhil, 1994). In these models the bottom shear stress τ_b on the flow is normally assumed to depend on the depth-averaged velocity squared:

$$\tau_b = -\rho u_* |u_*| = -\rho c_f U |U| \quad (5)$$

in which u_* is the friction velocity, U the streamwise depth-averaged velocity component (the dominating component in shallow mixing layers), and $c_f = (u_*/U)^2$ the bottom-friction coefficient, which depends slightly on the wall roughness or on U in case of a hydraulically smooth bottom.

Besides its influence on the main flow the bottom friction influences the development of a shallow mixing layer. The bottom friction has a stabilizing influence on the generation of large-scale turbulence due to transverse shear, because the horizontal, large-scale motions are obstructed by the bottom shear stresses. In other words the bottom friction suppresses the effective production of transverse-shear induced-turbulence. This suppression results in a reduction of the spreading rate of a shallow mixing layer. This stabilizing effect can be expressed in terms of a dimensionless stability number S , the bed-friction number (Chu and Babarutsi, 1988).

$$S \equiv \frac{c_f \delta}{h} \frac{U_c}{\Delta_u} = \frac{c_f \delta}{2h\lambda} \quad (6)$$

with Δ_u the depth-averaged velocity difference across the shallow mixing layer, and U_c the depth-averaged centre velocity, defined in a similar way as Δ_u and u_c . Above a certain critical value of the bed-friction number S_{crit} the effective production of large-scale turbulence vanishes and the growth of the mixing layer stops virtually, but for a very small effect of the bottom turbulence. Theoretical critical values calculated on the basis of a stability analysis of parallel flows are 0.06 (Alavian and Chu, 1985) and 0.12 (Chu et al., 1991).

Measured data of shallow mixing layers presented by Chu and Babarutsi (1988) show a linear dependence of the spreading coefficient α on the bed-friction number S . Based on these data they suggest the following relation between α and S

$$\alpha = \alpha_0 \left(1 - \frac{S}{S_{\text{crit}}} \right) \quad \text{for } S < S_{\text{crit}} \quad (7)$$

$$\alpha = 0 \quad \text{for } S > S_{\text{crit}}$$

Here the subscript $_0$ denotes the initial value of the corresponding variable at the origin of the mixing layer, making α_0 the initial spreading coefficient.

A developing shallow mixing layer can be divided in three regions depending on dominating flow characteristics.

- *Near field*: Downstream from the splitter plate the width of the layer is initially smaller than the water depth and the influence of the bottom on the mixing layer is small. In this region the flow develops as a free mixing layer. However, the bottom turbulence present in the ambient flow can lead to a slightly higher initial spreading rate.
- *Middle field*: The bottom friction has a major influence on the development of the mixing layer, leading to a decrease of the spreading rate. Here, large horizontal eddies develop with dimensions larger than the water depth.
- *Far field*: The horizontal large-scale eddies have dimensions much larger than the water depth. The stabilizing influence of the bottom friction suppresses the generation of new large-scale eddies, leading to an almost zero-growth of the mixing layer.

The bottom friction reduces the growth of the shallow mixing layer not only by suppressing the large-scale structures but also in another way. The bottom shear stress working on the fast stream is larger than the one working on the slow stream due to the difference in the mean velocity. As the longitudinal gradient of the free surface slope, which yields the driving force on the main flow, hardly varies in the transverse direction, the fast stream is decelerated, and the slow stream is accelerated. This phenomenon results in a decrease of the transverse velocity difference across the mixing layer, which in turn leads to a decrease of the spreading rate (see eq. 2).

Because of conservation of mass the decelerating fast ambient stream widens and the accelerating slow ambient stream narrows. The space in which shallow mixing layers develop in the natural environment is generally confined (the width of the river, the distance to the shore). The deceleration of the fast ambient stream and the acceleration of the slow ambient stream then lead to a

displacement of the (centre of the) mixing layer to the side of the slow ambient stream. The same process influences the exact profile of the mixing layer. The faster side of the mixing layer is decelerated and widens and the slower side is accelerated and narrows, leading to a slight asymmetry in the profile of the mixing layer. Measurements with a laser-Doppler velocimeter (LDV) by Uijttewaal and Booij (2000) show a slight deviation of the error-function profile, especially in the middle field of the shallow mixing layer. The profiles are not completely similar (see figure 2), which is not surprising as now more than one length scale, the width of the mixing layer and the water depth, play a role. However, the deviation is so small that for modelling purposes the error-function profile can be retained.

4. Integral model of shallow mixing layers

To predict the development of mixing layers in shallow flows a simple integral model was developed. The model is based on the shallow water equations, which are integrated over the transverse direction. This transverse integration is executed for three regions separately: the fast ambient stream, the mixing layer and the slow ambient stream. The aim of the model is to estimate the downstream evolution of the width of the mixing layer and the transverse displacement.

Shallow-water flows are characterised by a restricted water depth, which is much smaller than the horizontal length scales of motion. Vertical accelerations can normally be neglected and a hydrostatical pressure distribution over the vertical assumed. Integration over the water depth h of the three-dimensional mass and momentum transport equations yields the shallow-water equations. Details of this integration procedure are given by Vreugdenhil (1994). For stationary flows and neglecting Coriolis accelerations and horizontal external forces, the shallow-water equations are:

$$\frac{\partial(hU)}{\partial x} + \frac{\partial(hV)}{\partial y} = 0 \quad (8)$$

$$\frac{\partial(hU^2)}{\partial x} + \frac{\partial(hUV)}{\partial y} - \frac{\partial(hT_{xy})}{\partial y} = -gh \frac{\partial z_f}{\partial x} - c_f U^2$$

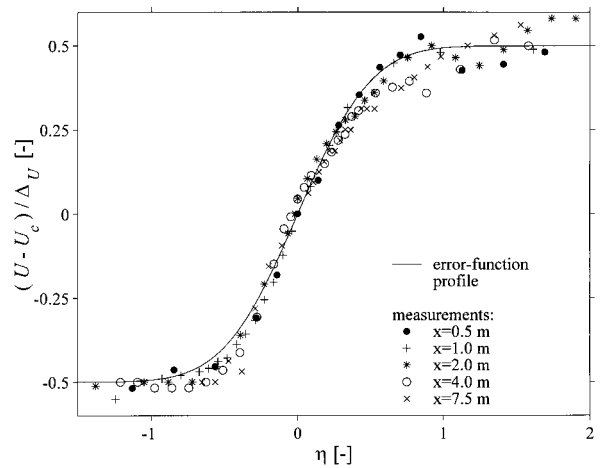


Fig. 2. Deviation of the error-function profile in a very shallow mixing layer ($h = 42$ mm).

The transport equation for the transverse component of the momentum plays only a minor role as $V \ll U$, with V the depth-averaged transverse velocity, and is omitted. In eq. (8) z_f is the vertical coordinate of the free surface, $z_f = h + z_b$, with z_b the vertical coordinate of the bottom. The depth-averaged shear stress T_{xy} includes the viscous stress, the turbulent or Reynolds stress, and a differential advection term (Vreugdenhil, 1994). In quasi-two-dimensional shear layers, such as in shallow mixing layers, the transverse turbulent shear stress dominates. A depth-averaged normal stress term T_{xx} is neglected in eq. (8).

To obtain the integral (1-dimensional) model the shallow-water equations are integrated over the transverse direction. In the integral model the flow is divided in three regions, namely a fast ambient stream ($y_1 \leq y < y_{1w}$), a mixing-layer region ($y_2 < y < y_1$) and a slow ambient stream ($y_{2w} < y \leq y_2$), see figure 3. Mixing layers in laboratory flumes and in the environment develop in flows of limited width. The transverse coordinates y_{1w} and y_{2w} give the positions of the side-walls on the fast-stream and slow-stream side respectively. The coordinates y_1 and y_2 present the positions of the internal boundaries between the mixing-layer region and the ambient streams regions, $y_1 = y_c + 1/2 b_m$ and $y_2 = y_c - 1/2 b_m$. The width of the mixing layer region is $b_m = y_1 - y_2 = \beta \delta$ where β should be chosen large enough for the mixing layer region to include the

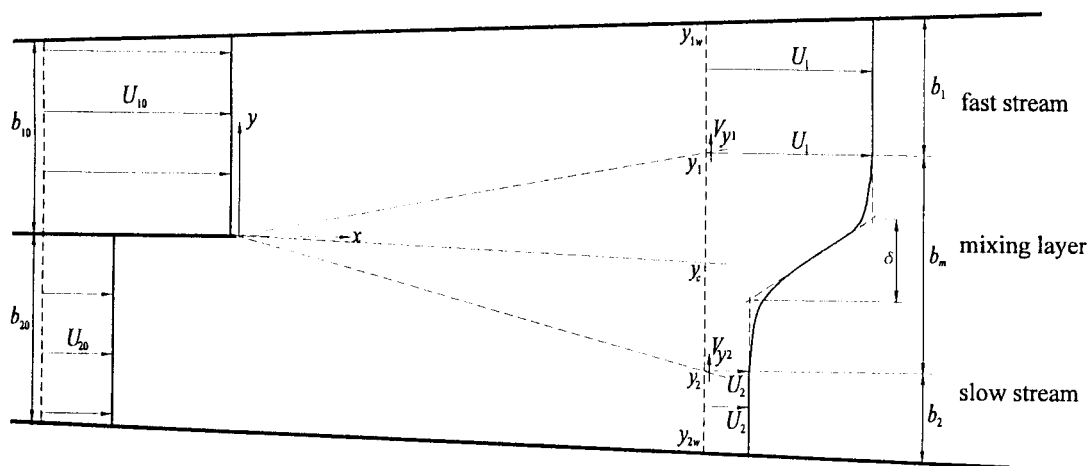


Fig. 3. Scheme of a laterally confined shallow mixing layer.

layer with considerable shear and small enough to remain between the sidewalls. Hence the model is only applicable when the sidewalls are far enough to not interfere with the development of the mixing layer, leaving ample room for ambient streams. The coordinates y_1 and y_2 depend on the spreading rate and displacement rate of the mixing-layer region, and are therefore a function of the streamwise coordinate x . The shallow water equations are integrated for each region separately.

The boundary conditions of this model with regard to the sidewalls and internal boundaries are as follows: there is no flow across the side-walls and the influences of the boundary layers along the side-walls are neglected ($T_{xy}=0$). The internal boundaries between the mixing layer region and the ambient streams are chosen far from the mixing layer centre. Therefore the flow conditions at the internal boundaries y_1 and y_2 can be approximated with the conditions in the ambient streams: $U = U_1$ and $T_{xy}=0$ at y_1 ; $U = U_2$ and $T_{xy}=0$ at y_2 . The internal boundary conditions for the transverse velocities V are $V=V_{y1}$ (at $y = y_1$) and $V=V_{y2}$ (at $y = y_2$). For the ambient streams the transverse profiles of the longitudinal velocity U are assumed to be uniform, with $U = U_1$ for the fast stream and $U = U_2$ for the slow stream. Because the transverse mean velocity component V is much smaller than the longitudinal component U the transverse slope of the free surface can be neglected in relation to the longitudinal slope. Hence in the model the free surface level z_f is considered constant in a cross-section, as are the bottom level z_b and hence the water depth h . Integration over the transverse direction of the shallow-water equations yields a set of two integral 1D-equations for each region. The integral equations for the mixing layer region depend on the profile function of U , hence they are written as transverse integrals of U in terms of the profile function $f(\eta)$. The obtained 1D-equations describe the evolution of the mean velocity of the ambient streams U_1 and U_2 , of the water depth h and of the displacement of the layer centre y_c . The result of the integration of the mass equation for the fast stream, the slow stream and the mixing layer regions, is respectively:

$$\begin{aligned} b_1 h \frac{dU_1}{dx} + b_1 U_1 \frac{dh}{dx} - h V_{y1} + h U_1 \frac{dy_{1w}}{dx} &= 0 \\ b_2 h \frac{dU_2}{dx} + b_2 U_2 \frac{dh}{dx} + h V_{y2} - h U_2 \frac{dy_{2w}}{dx} &= 0 \\ h I'_U + I_U \frac{dh}{dx} + h V_{y1} - h V_{y2} &= 0 \end{aligned} \quad (9)$$

with $b_1=y_{1w}-y_1$ and $b_2=y_2-y_{2w}$ the widths of the ambient flow regions and I_u and I'_u transverse integrals of U defined below. The integral streamwise momentum equations of the fast stream, the slow stream and the mixing layer are respectively

$$\begin{aligned} h U_1 \frac{dU_1}{dx} &= -g h \frac{d(h+z_b)}{dx} - c_{f1} U_1^2 \\ h U_2 \frac{dU_2}{dx} &= -g h \frac{d(h+z_b)}{dx} - c_{f2} U_2^2 \\ h I'_{UU} + I_{UU} \frac{dh}{dx} + h U_1 V_{y1} - h U_2 V_{y2} &= -g b_m h \frac{d(h+z_b)}{dx} - c_{fm} I_{UU} \end{aligned} \quad (10)$$

where the integral momentum equations for the fast and the slow stream regions are simplified by the substitution of the integral mass equations and division through b_1 and b_2 respectively. The parameters c_{f1} , c_{f2} and c_{fm} are the bottom friction coefficients of the fast and the slow ambient flow and the mixing layer respectively.

The transverse integrals of U in equations (9) and (10) are:

$$\begin{aligned} I_U &\equiv \int_{y_2}^{y_1} U \, dy = b_m \left[U_c + \Delta_U \frac{I_f}{\beta} \right]; \\ I'_U &\equiv \int_{y_1}^{y_2} \frac{dU}{dx} \, dy = b_m \frac{dU_c}{dx} - \Delta_U \frac{dy_c}{dx} + \frac{db_m \Delta_U}{dx} \frac{I_f}{\beta}; \\ I_{UU} &\equiv \int_{y_1}^{y_2} U^2 \, dy = b_m \left[U_c^2 + 2 U_c \Delta_U \frac{I_f}{\beta} + \Delta_U^2 \frac{I_{ff}}{\beta} \right]; \\ I'_{UU} &\equiv \int_{y_1}^{y_2} \frac{dU^2}{dx} \, dy = 2 b_m U_c \frac{dU_c}{dx} - 2 U_c \Delta_U \frac{dy_c}{dx} \\ &\quad - \frac{1}{4} \Delta_U^2 \frac{db_m}{dx} + 2 \frac{db_m U_c \Delta_U}{dx} \frac{I_f}{\beta} + \frac{db_m \Delta_U^2}{dx} \frac{I_{ff}}{\beta} \end{aligned} \quad (11)$$

in which I_f and I_{ff} are integrals of the profile function $f(\eta)$ defined as

$$I_f \equiv \int_{\eta_2}^{\eta_1} f(\eta) \, d\eta; \quad I_{ff} \equiv \int_{\eta_2}^{\eta_1} f^2(\eta) \, d\eta \quad (12)$$

Substitution of the error-function profile for $f(\eta)$ (eq. 4) and $\beta=b_m/\delta$ yields $I_f = 0$ (as it does for all point-symmetric profile functions) and $I_{ff} = \frac{1}{4}\beta - (\pi\sqrt{2})^{-1}$ if η_1 and η_2 go to ∞ and $-\infty$ respectively.

In equations (11) U_c and Δ_U are used for shortness of notation. Substitution of $U_c = \frac{1}{2}(U_1 + U_2)$ and $\Delta_U = (U_1 - U_2)$ gives the integral 1D-model for the streamwise evolution of a shallow mixing layer between two parallel streams. The model consists of a set of six equations: three integral mass equations (9) and three integral momentum equations (10). This set of (non-linear, first order) differential equations can be evaluated numerically, with as variables U_1 , U_2 , V_{y1} , V_{y2} , h , and y_c . The mixing layer width $b_m = \beta\delta$ is obtained by means of the semi-empirical relation for the spreading rate, see equations (2) and (7)

$$\frac{db_m}{dx} = \beta \alpha_0 \lambda \left(1 - \frac{S}{S_{crit}} \right) \text{ for } S < S_{crit}; \quad \frac{db_m}{dx} = 0 \text{ for } S > S_{crit} \quad (13)$$

and the widths of the ambient streams b_1 and b_2 by the algebraic expressions $b_1 = y_{1w} - y_c - \frac{1}{2}b_m$ and $b_2 = y_c - y_{2w} - \frac{1}{2}b_m$. In the model the position of the side-walls y_{1w} and y_{2w} and the bottom level z_b are required, as are values for the initial spreading coefficient α_0 , for the integrals of the profile functions I_f and I_{ff} and for the coefficient β defining the width of the mixing region and expressions or values for the bottom friction coefficients.

The required initial conditions are values for both inlet velocities and widths of the ambient streams, and for the water depth. A non-zero initial mixing layer width is required. Its value can be related to the physical situation at the origin of the mixing layer: e.g. the thickness of the splitter plate or of the boundary layers along the splitter plate. The transverse boundary velocities V_{y1} and V_{y2} can be assumed to have an initial value of zero. The model yields the development of the mixing layer width, together with the evolution of the water level, of the velocities and widths of the two ambient flows, of the displacement of the mixing layer centre and the transverse boundary velocities.

5. Experiments

To evaluate the integral model the development of shallow mixing layer flows with different inflow conditions was investigated in the shallow-water flume of the Laboratory for Fluid Mechanics of the Delft University of Technology. The flume has a length of 20 m, a width of 3 m and a height of 0.2 m. It is designed for the investigation of large horizontal turbulence structures in shallow flows. To this end the relatively wide and shallow flume has a horizontal glass bottom to allow LDV-measurements from below. To generate a mixing layer flow, the inlet region is divided into two equal sections by a glass splitter plate with a thickness of 4 mm and a length of 3 m. Downstream of the splitter plate a mixing layer develops. The long inlet region guarantees that the inlet streams have a developed bottom boundary layer at the end of the splitter plate.

Before the proper LDV-experiments the shallow-water flume was used to investigate the development of shallow mixing layers (Tukker, 1997). To this end transverse profiles of the streamwise velocity were measured with an array of micro-impellers. The transverse coordinates of the impellers are $y = -1.30, -1.00, -0.70, -0.40, -0.205, -0.055, 0.055, 0.205, 0.40, 0.70, 1.00$ and 1.30 m. The streamwise coordinates of the cross-sections at which the velocity profiles were measured are $x = 0, 3, 6, 9, 12$ and 15 m. The origin ($x = 0, y = 0$) coincides with the end of the splitter plate, i.e. the origin of the mixing layer. The impellers were placed near the free surface with the centre of each impeller at about $.8h$. The depth averaged velocity U is about 10% smaller than the velocity measured at this level.

The micro-impeller used is designed to measure the velocity in small ducts and hydraulic models. In essence it is a small plastic propeller with a diameter of 15 mm, which is driven by the flow. The angular speed is a measure for the velocity of the flow. The impellers have different threshold or starting velocities between about 0.02 m/s and 0.10 m/s. The specified measuring accuracy is about 5 mm/s. However the performance of the impellers easily deteriorates as a result of pollution (dust, etc.) of the propellers and their bearings. Because of its dimensions an impeller measures a velocity averaged over an area with a diameter of about 15 mm, which can lead to errors in thin mixing layers and in very shallow flow. Another error source in very shallow flow is the small distance of the impeller to the bottom and the water surface, which may lead to a disturbed flow pattern around the probe. The measuring time in a single point was about 600 s and the corre-

sponding number of samples 6000. Time-averaging of the velocity data and a correction for the probe level yielded the measured depth-averaged streamwise velocities U . From the obtained velocity profile in a cross-section measured values for U_1, U_2 (or Δ_U and U_c), δ and y_c were estimated.

The water level was measured with a point gauge which gives a precision of about .5 mm for the measured water levels in a flow, which is rather low considering the small surface slopes in the experiments. The measurements show a nearly constant water level in a cross-section, as assumed in the integral model of shallow mixing layers.

The flume is a model of the confluence of two rivers, hence the flow in the flume should be sub-critical (i.e. have a Froude-number, $Fr = U/(gh)^{1/2}$, smaller than unity) and have a fully developed bottom turbulence (i.e. have a Reynolds number, $Re = Uh/\nu$, larger than 2000, where ν is the kinematic viscosity). The two conditions of turbulent flow and sub-critical flow restrict the possible inlet flow conditions. The development of the mixing layer was investigated in four flow cases that satisfy those conditions everywhere, using .5 as an upper limit for Fr and 4000 as a lower limit for Re . The inlet conditions of the four cases are summarized in table 1.

Table 1. The inlet conditions, denoted by the subscript $_0$, of the four shallow mixing layer cases.

case	$(U_1)_0$ [m/s]	$(U_2)_0$ [m/s]	$(\Delta_U)_0$ [m/s]	$(U_c)_0$ [m/s]	h_0 [m]
A	0.238	0.118	0.120	0.178	0.052
B	0.304	0.142	0.162	0.223	0.098
C	0.319	0.072	0.247	0.196	0.077
D	0.264	0.082	0.182	0.173	0.059

Earlier measurements by Chu and Babarutsi (1988) are less useful for the evaluation of the model. In their experimental setup the much shorter splitter plate (1.22 m) was located in the contraction region of the flow. This led to less well adjusted inlet flow and to a near doubling of the initial mixing layer growth, $\alpha_0 \approx .36$ (Uijtewaal and Tukker, 1998). Moreover the flume was not of sufficient width, .61 m, to accommodate both ambient streams.

6. Results of the integral model

To evaluate the integral model computations of the development of shallow mixing layer flows for the four flow cases were executed. The required start conditions are the inlet velocities, $(U_1)_0$ and $(U_2)_0$, and inlet widths, $(b_1)_0$ and $(b_2)_0$, of both ambient streams, the inlet water depth $(h)_0$ and the initial width of the mixing layer region at the end of the splitter plate $(b_m)_0$. Of those $(U_1)_0, (U_2)_0$, and $(h)_0$ follow from table 1. The three widths, $(b_1)_0, (b_2)_0$ and $(b_m)_0$ follow from the layout of the flume and from an estimate of the thickness of the boundary layer along the splitter plate. Uijtewaal and Tukker (1998) suggest a virtual origin of the

mixing layer, $x_o \approx -.25$ m, based on extensive measurements in the near field region of a shallow mixing layer. This corresponds to an initial mixing layer width $(b_m)_0 = 0.25 \beta \alpha_0 \lambda_0$ m.

Several constants in the model have to be set, α_0 , the initial spreading coefficient, S_{crit} , the critical bed-friction number, β , the constant determining the width of the mixing layer region and I_f and I_{ff} , integrals of the profile function. Assumption of an error profile determines I_f and I_{ff} (see ch. 4) and with $\beta = 1.9$, the error in the velocity at the boundary of the mixing layer region remains small, a deviation of only 1% of Δ_U for this profile. Based on their measurements Uijtewaal and Tukker (1998) estimate $\alpha_0 \approx 0.20$. Finally a value for $S_{crit} = .07$ gave the best results. This lies well in the range deduced theoretically (see ch. 3). Moreover a variation of 10% in the value of α_0 or 20% in the value of S_{crit} hardly changes the results of the model.

For the straight flume with horizontal bottom dy_{1w}/dx , dy_{2w}/dx and dz_b/dx in equations 9 and 10 disappear. The bottom friction coefficients c_{f1} and c_{f2} in the two ambient flows over the hydraulically smooth glass bottom are obtained from

$$\frac{1}{\sqrt{c_f}} = \frac{1}{\kappa} [\ln (.11 Re \sqrt{c_f}) - 1.0] \quad (14)$$

(derived for a logarithmic vertical velocity profile with a roughness coefficient $z_0 = .11\nu/u_*$), in which κ is the Von-Karman con-

stant ($\kappa = .4$) and Re the Reynolds number of the considered ambient flow. This yields c_f -values of the order of .003 for both ambient flows in all cases considered here. For the friction coefficient for the mixing layer the mean value $c_{fm} = 1/2(c_{f1} + c_{f2})$ is used.

In the figures presented in this chapter the numerical results of the integral model for shallow mixing layers are compared to the measurements. Figure 4 shows the evolution of the depth-averaged centre velocity U_c and of the depth-averaged velocity difference Δ_U for all four cases. Figure 5 shows the depth h , and figure 6 the position of the centre of the mixing layer y_c as a function of the distance to the origin of the mixing layer, x . In view of the simplicity of the model these variables are reproduced satisfactory. The measured and computed values for the ambient velocities agree well generally. The large error in the measurements of the water level exclude a better fit between computation and measurements. Deviations and errors in the measured velocity profile lead to errors in the determination of the measured centre of the mixing layer, which in particular impairs the measured y_c in very shallow flow (case A).

The depth-averaged centre velocity U_c hardly changes with x . This is due to the special layout of the flume, with equal inlet widths of the ambient flows and a relatively small displacement of the centre of the mixing layer compared to the large total width. Hence U_c is a good measure for the average velocity in the cross-section, which varies hardly because of the slow decrease of h .

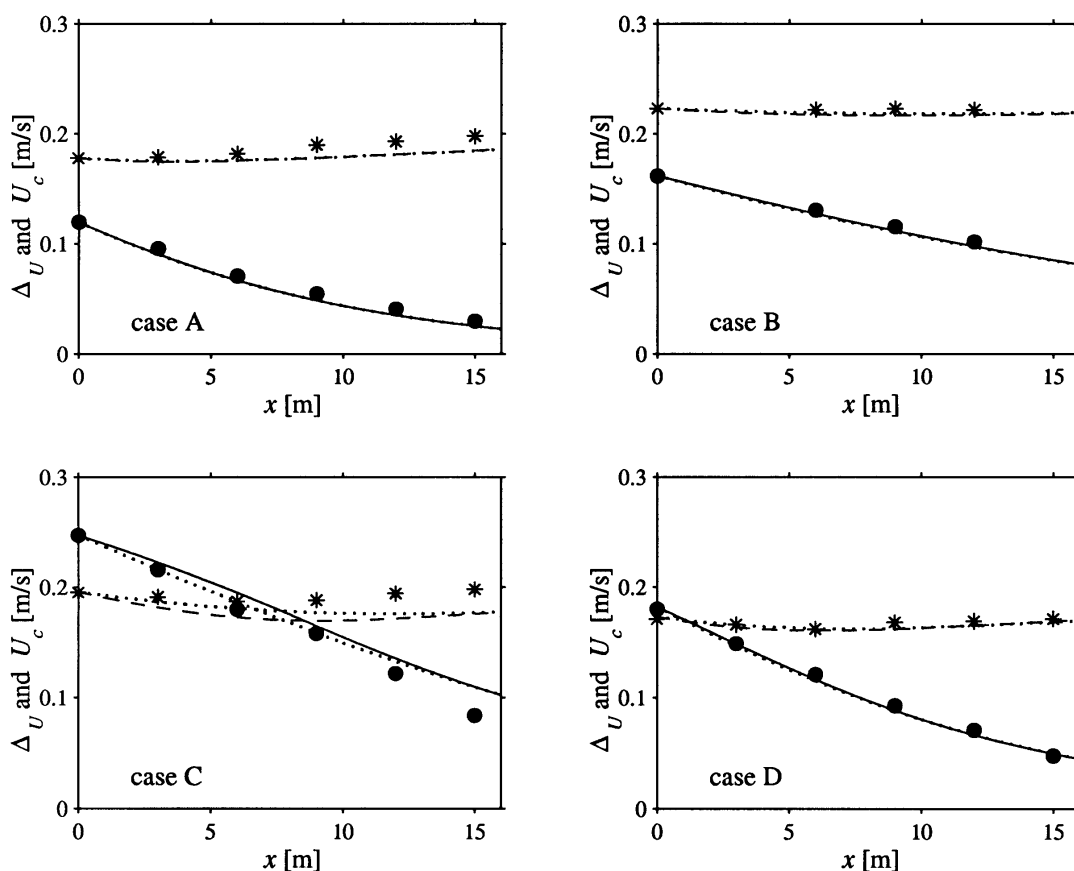


Fig. 4. Downstream evolution of the velocity difference, Δ_U , and the mean convection velocity, U_c , (for cases A, B, C and D): measurements Δ_U (•) and U_c (*), computation Δ_U (—) and U_c (---), computation without a mixing layer ($\alpha = 0$) , x is the distance to the origin of the mixing layer.

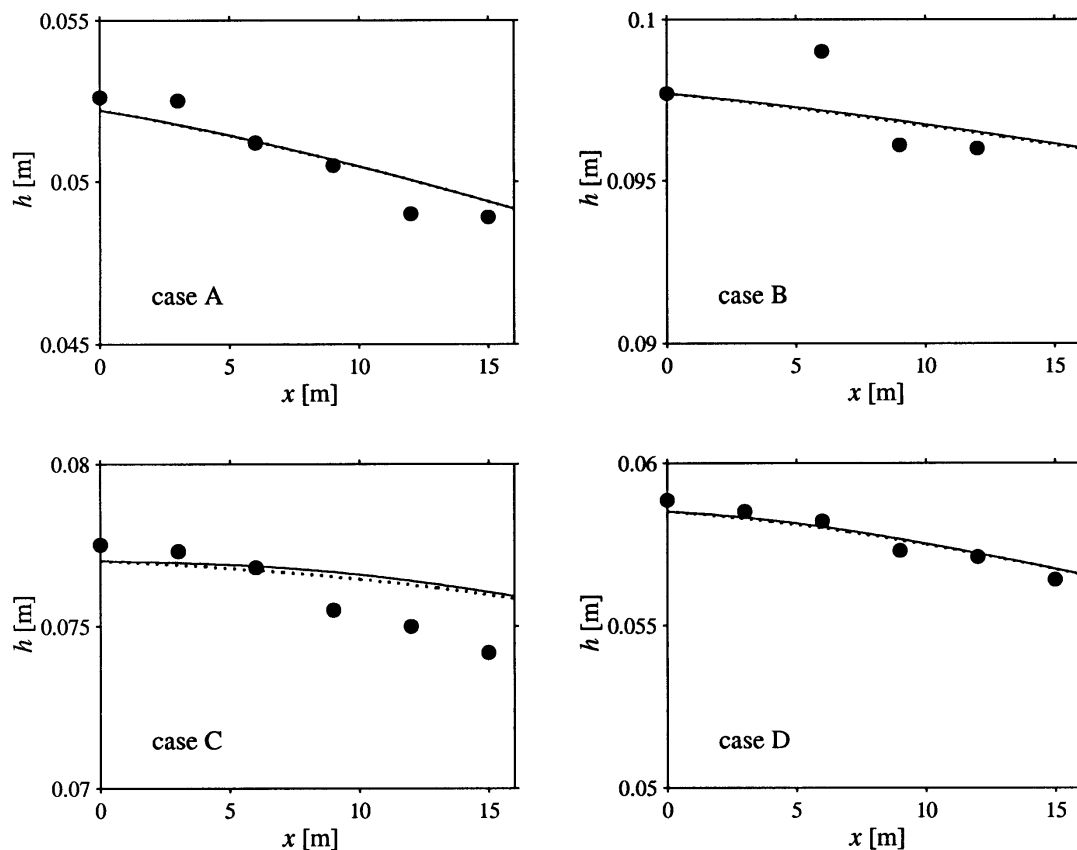


Fig. 5. Downstream decrease of water depth, h , (for cases A, B, C and D): • measurements, — computation (..... computation with $\alpha = 0$), x is the distance to the origin of the mixing layer.

The evolutions of U_c , ΔU , y_c and h are hardly influenced by the development of the mixing layer. This is shown by the dotted lines in figures 4 to 6 which show the results of computations without a developing mixing layer (by setting α to 0). These dotted lines deviate only slightly from (and are often completely covered by) the lines that represent the computations with a mixing layer. The evolution of these quantities is mainly determined by the bottom friction on the main flow, which results in an equalization of the velocities in the ambient streams.

Figure 7 shows the downstream development of the mixing layer width, δ . A correct reproduction of δ and of the velocity difference across the mixing layer, ΔU , are important as they determine the coefficient for lateral diffusion and so the exchange of matter between both flows. Figure 7 shows that the reproduction of δ is satisfactory. Again the errors in the measured velocity profiles for the very shallow flow (case A) obviously lead to a wrong measured mixing layer width. As discussed in chapter 3 the bottom friction reduces the growth of the shallow mixing layer in two ways. First it reduces the velocity difference, ΔU , and second it suppresses the large scale structures. Both effects can be implemented separately in the model. In figure 7 results of computations without a bottom friction effect (the deep water case with $\lambda = \lambda_0$ and $S_{crit} = \infty$, leading to a linear growth of the mixing layer), computations with only the suppression of the large scale structures ($\lambda = \lambda_0$ but $S_{crit} = .07$) and computations with only the decrease in the velocity difference ($S_{crit} = \infty$) are added. It is clear that both effects play a role. In particular cases C and D show that

the mixing layer width reaches an asymptotic value in the far field (while $S \Rightarrow S_{crit}$), despite the continued presence of a velocity difference across the mixing layer.

The exact form of the velocity profile of the mixing layer appears not to play an important role. Computations with a linear profile ($f(\eta)=\eta$ for $-1/2 < \eta < 1/2$, $f(\eta)=-1/2$ for $\eta < -1/2$, $f(\eta)=1/2$ for $\eta > 1/2$ in equation 3 with $\beta=1$, $I_f=0$ and $I_{ff}=1/12$) lead to indistinguishable results not shown in figure 4-7. The small deviation of the error profile in shallow mixing layers can hence be neglected.

As the shallow mixing layers in flumes were reproduced satisfactory, the integral model was used to predict the development of the mixing layer in a river confluence. Secondary flow, depth differences, etc. (Biron et al. 1996) were left out of consideration. Five cases were considered, see table 2, with case 1 the basic situation. In case 2 and 3 the velocity difference between both rivers is raised to a very high value. In case 4 and 5 the width ratio of both rivers is changed. All five cases have an equal and uniform bottom friction coefficient c_f and a uniform slope of the riverbed $i=dz_b/dx$. This slope should be not too far from the equilibrium slope for the considered c_f and average velocity. Otherwise the development of the merged river can become unstable as all boundary conditions are given as inflow conditions in the model which is not recommended for a sub-critical flow. Figure 8 gives the results.

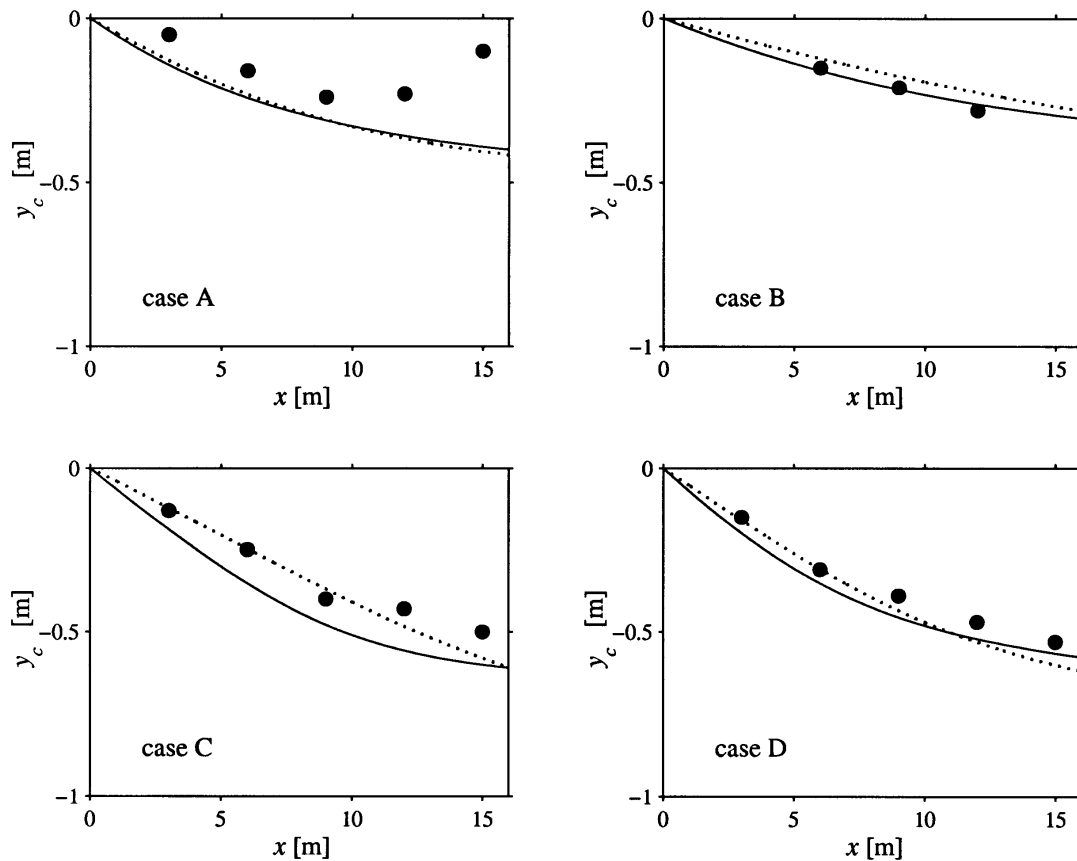


Fig. 6. Transverse displacement of mixing layer centre, y_c , (for cases A, B, C and D): • measurements, — computation (..... computation with $\alpha = 0$), x is the distance to the origin of the mixing layer.

Table 2. Properties of the five computed river confluences.

case	$(U_1)_0$ [m/s]	$(U_2)_0$ [m/s]	$(b_1)_0$ [m]	$(b_2)_0$ [m]	i	c_f	h_0 [m]
1	1.4	0.8	100	200	.0025	.005	2
2	2.0	0.5	100	200	.0025	.005	2
3	2.5	0.25	100	200	.0025	.005	2
4	1.4	0.6	150	150	.0025	.005	2
5	1.4	0.92	50	250	.0025	.005	2

A remarkably short development length and small width of the mixing layer is apparent. The width amounts to only a few depths, except for the cases with very large velocity differences between the rivers. The very narrow mixing layers correspond to very low exchanges of material between the merged rivers, which is often observed in nature between rivers with distinct colours. This low exchange can have important consequences for the transport of sediment or pollutants. The influence on the longitudinal dispersion may be dramatic.

7. Conclusions

Bottom friction restricts the development of shallow mixing layers in two ways: It suppresses the large-scale turbulent structures in the mixing layer and it leads to a decrease of the velocity dif-

ference between both ambient flows. To predict the development of mixing layers in shallow flows a simple integral model was developed in which both reduction mechanisms are incorporated. The development of shallow mixing layers was investigated in a shallow water flume to evaluate the model.

Comparison of the evolutions of centre velocity, U_c , the velocity difference across the mixing layer, Δ_U , the position of the mixing layer centre, y_c , the water depth, h , and the mixing layer width, δ , between model results and measurements was executed. The model gives a fair reproduction of the downstream evolution of all five quantities. The evolutions of the four first quantities, U_c , Δ_U , h and y_c , appear to be hardly influenced by the development of the mixing layer. They are mainly determined by the bottom friction on the main flow, which results in an equalization of the velocities in the ambient streams.

The momentum exchange through the mixing layer appears to play a minor role in the equalization of the velocities of the ambient streams. In the momentum equations the momentum source by the surface slope and the momentum sink by bottom friction are dominant. Exchange of matter can however only take place through the mixing layer and the evolution of the sediment or pollutant content of the ambient streams is hence determined by the development of the mixing layer.

Figure 7 shows the downstream development of the mixing layer width, δ . A correct reproduction of δ and of the velocity difference across the mixing layer, Δ_U , is important as they determine the coefficient for lateral diffusion and therewith the exchange of

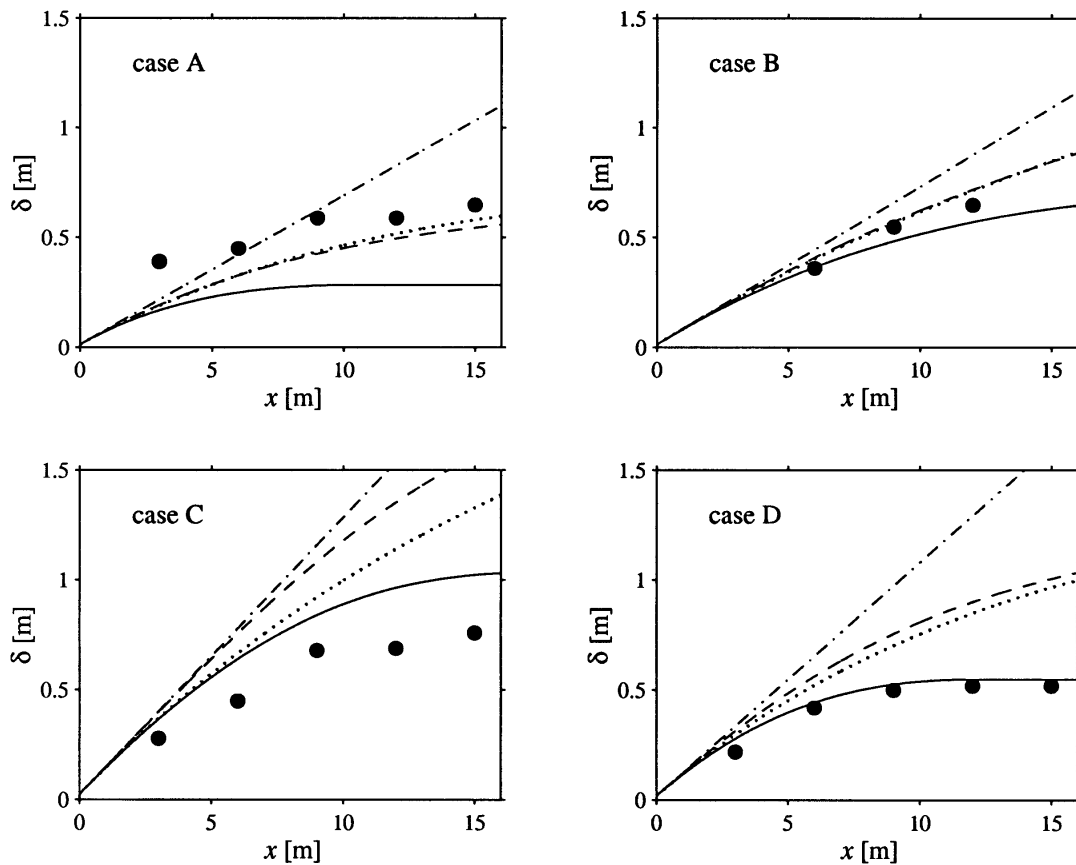


Fig. 7. Downstream evolution of mixing layer width, δ , (for cases A, B, C and D): • measurements, — computation, (other computations: - - - $S_{crit} = \infty$, $\lambda = \lambda_0$, -.-.- deep water case), x is the distance to the origin of the mixing layer.

matter between both flows. The computations show that both effects of the bottom friction on the growth of the mixing layer are important and that they together determine an asymptotic width of the mixing layer in the far field. In shallow mixing layers the velocity profile deviates slightly from the error profile. However the exact form of the velocity profile of the mixing layer appears not to play an important role.

Simulation of river confluences yields remarkably small mixing layer widths of only a few depths generally. The very narrow mixing layers correspond to very low exchanges of material be-

tween the merging rivers, which often remain distinct far downstream of the confluence. The low exchange is of importance for the transport of sediment or pollution and for the longitudinal dispersion in rivers.

References

ALAVIAN, V., and V.H. CHU, 1985, *Turbulent exchange flow in shallow compound channel*, Proceedings 21th IAHR Congress, Melbourne, Vol. 3. pp. 446-451.

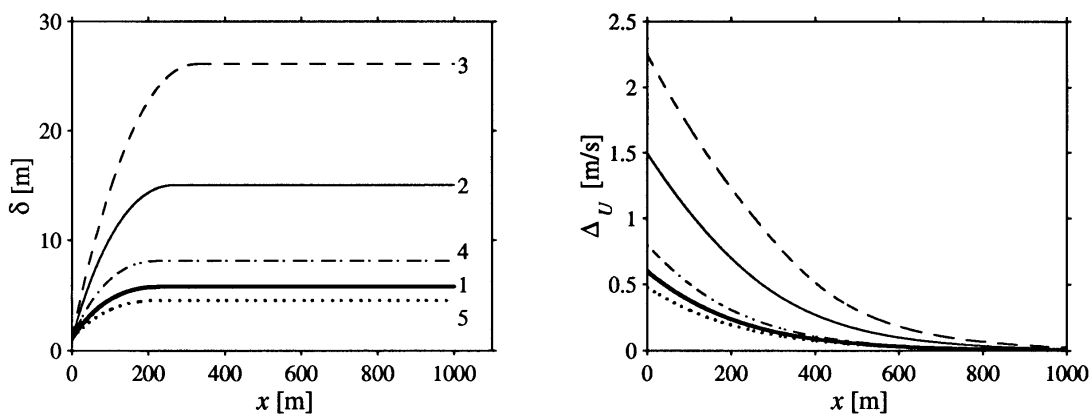


Fig. 8. Computed development of the mixing layers in river confluences: mixing layer width, δ , and velocity difference, ΔU , x is the distance to the origin of the mixing layer.

- BIRON, P., ROY, A.G., and BEST, J.L., 1996, *Turbulent flow structure at concordant and discordant open-channel confluences*, Exp. in Fluids, Vol. 21, pp. 437-446.
- BROWN, G.L. and A. ROSHKO, 1974, *On density effects and large structure in turbulent mixing layers*, Journal of Fluid Mechanics, Vol. 64, part 4, pp. 775-816.
- CHEN, D., and JIRKA, G.H., 1995, *Experimental study of plane turbulent wakes in a shallow water layer*, Fluid Dynamics Research, Vol. 16, pp. 11-41.
- CHU, V.H. and S. BABARUTSI, 1988, *Confinement and Bed-Friction Effects in Shallow Turbulent Mixing Layers*, Journal of Hydraulic Engineering, Vol. 114, No. 10, pp. 1257-1274.
- CHU, V.H., J.-H. WU and R.E. KHAYAT, 1991, *Stability of Transverse Shear Flows in Shallow Open Channels*, Journal of Hydraulic Engineering, Vol. 117, No. 10, pp. 1370-1388.
- DRACOS, Th., M. GIGER and G.H. JIRKA, 1992, *Plane turbulent jets in a bounded fluid layer*, Journal of Fluid Mechanics, Vol. 241, pp. 587-614.
- GÖRTLER, H. 1942, *Berechnung von Aufgaben der freien Turbulenz auf Grund eines neuen Näherungsansatzes*, Zeitschrift für angewandte Mathematik und Mechanik, Vol. 22, No. 5, pp 244-254. (in German)
- KNIGHT, D.W. and K. SHIONO, 1990, *Turbulence measurements in a shear layer region of a compound channel*, Journal of Hydraulic Research, Vol. 28, No. 2, pp. 175-196.
- LANGENDOEN, E.J., 1992, *Flow Patterns and Transport of Dissolved Matter in Tidal Harbours*, dissertation, Delft University of Technology, Department of Civil Engineering.
- LLOYD, P.M., and STANSBY, P.K., 1997, *Shallow-water flow around model conical islands of small side slope*, J. Hydr. Res., Vol. 123, No. 12, pp.1057-1077.
- PUI, N.K., and I.S. GARTSHORE, 1979, *Measurements of the growth rate and structure in plane turbulent mixing layers*, Journal of Fluid Mechanics, Vol. 91, part 1, pp. 111-130.
- SELLIN, R.H.J., 1964, *A laboratory investigation into the interaction between the flow in the channel of a river and that over its flood plain*, La Houille Blanche, Vol. 19, No 7, pp. 793-801.
- TOWNSEND, A.A., 1976, *The structure of turbulent shear flow*, second edition (first edition: 1956), Cambridge University Press, Cambridge.
- TUKKER, J., 1997, *Turbulence structures in shallow free-surface mixing layers*, dissertation, Delft University of Technology, Department of Civil Engineering.
- UIJTTEWAAL, W.S.J, and TUKKER, J., 1998, *Development of quasi two-dimensional structures in a shallow free-surface mixing layers*, Exp. Fluids, Vol. 24, pp.192-200.
- UIJTTEWAAL, W.S.J, and BOOIJ, R., 2000, *Effects of shallowness on the development of free-surface mixing layers*, Physics of Fluids, Vol. 12, No 2, pp. 392-402.
- VREUGDENHIL, C.B., 1994, *Numerical methods for shallow-water flow*, Water Science and Technology Library, Volume 13, Kluwer Academic Publishers, Dordrecht.